FEBS Letters 586 (2012) 1759–1764

FEBS Letters

journal homepage: www.FEBSLetters.org

Structural recognition mechanisms between human Src homology domain 3 (SH3) and ALG-2-interacting protein X (Alix)

Xiaoli Shi [a,b,c,d], Stephane Betzi [a,b,c], Adrien Lugari [a,b,c], Sandrine Opi [a,b,c], Audrey Restouin [a,b,c], Isabelle Parrot [e], Jean Martinez [e], Pascale Zimmermann [a,b,c], Patrick Lecine [f], Mingdong Huang [d], Stefan T. Arold [g,*,1], Yves Collette [a,b,c,*,1], Xavier Morelli [a,b,c,*,1]

[a] CNRS UMR 7258, INSERM U 1068, Centre de Recherche en Cancérologie de Marseille, Marseille F-13009, France
[b] Institut Paoli-Calmettes, Marseille F-13009, France
[c] Aix-Marseille Université, Marseille, France
[d] State Key Laboratory of Structural Chemistry, Fujian Institute of Research on the Structure of Matter, Chinese Academy of Sciences, 155 Yang Qiao Xi Lu, Fuzhou, Fujian 350002, China
[e] Institut des Biomolécules Max Mousseron (IBMM), UMR 5247 CNRS, Université Montpellier 1, Université Montpellier 2, cc17-03, Place Eugène Bataillon, 34095 Montpellier Cedex 5, France
[f] Baylor Institute for Immunology Research, INSERM UMR899, 3434 Live Oak Street, Dallas, TX 75024, USA
[g] Department of Biochemistry and Molecular Biology, Unit 1000, The University of Texas MD Anderson Cancer Center, 1515 Holcombe Boulevard, Houston, TX 77030-4009, USA

ARTICLE INFO

Article history:
Received 1 March 2012
Revised 23 April 2012
Accepted 9 May 2012
Available online 26 May 2012

Edited by Gianni Cesareni

Keywords:
Apoptosis-linked gene 2-interacting protein X (Alix)
Protein–protein interaction
Src homology 3 domain (SH3 domain)
Src family kinase (SFK)
NMR
SAXS

ABSTRACT

The functions of Src family kinases are tightly regulated through Src homology (SH) domain-mediated protein–protein interactions. We previously reported the biophysical characteristics of the apoptosis-linked gene 2-interacting protein X (Alix) in complex with the haemopoietic cell kinase (Hck) SH3 domain. In the current study, we have combined ITC, NMR, SAXS and molecular modeling to determine a 3D model of the complex. We demonstrate that Hck SH3 recognizes an extended linear proline-rich region of Alix. This particular binding mode enables Hck SH3 to sense a specific non-canonical residue situated in the SH3 RT-loop of the kinase. The resulting model helps clarify the mechanistic insights of Alix–Hck interaction.

Structured summary of protein interactions:
Hck physically interacts with **SAM68** by two hybrid (View interaction)
FynR96I physically interacts with **Alix** by two hybrid (View interaction)
Hck binds to **Alix** by pull down (View interaction)
Fyn physically interacts with **SAM68** by two hybrid (View interaction)
Hck and **Alix** bind by nuclear magnetic resonance (View interaction)
FynR96I and **Alix** bind by isothermal titration calorimetry (View Interaction: 1, 2)
FynR96I and **Alix** bind by nuclear magnetic resonance (View interaction)
FynR96I binds to **Alix** by pull down (View interaction)
Hck physically interacts with **Alix** by two hybrid (View interaction)
FynR96I and **Alix** bind by x ray scattering (View interaction)
Hck physically interacts with **NEF** by two hybrid (View interaction)
FynR96I physically interacts with **NEF** by two hybrid (View interaction)

1. Introduction

Alix [ALG-2 (apoptosis-linked gene 2)-interacting protein X] is an adapter protein involved in normal and pathological cellular processes, including regulation of apoptosis, cytoskeletal dynamics, cell surface receptor internalization, endosomal sorting processes and virus budding from infected cell membranes [1–7]. These diverse functions appear to involve binding to various viral and cellular proteins (for review, refer to [8]), including kinases

Abbreviations: ALG-2, apoptosis-linked-gene-2; Alix, ALG-2 interacting protein X; EOM, ensemble optimization method; GST, glutathione S-transferase; Hck, haemopoietic; HSQC, heteronuclear single quantum coherence; ITC, isothermal titration calorimetry; PDB, protein data bank; PPII, polyproline type II; PRR, proline-rich region; SAXS, small-angle X-ray scattering; SFKs, Src family of non-receptor protein tyrosine kinases.

* Corresponding authors. Fax: +1 713 792 0855 (S.T. Arold); +33 491 26 03 64 (Y. Collette); +33 491 164 540 (X. Morelli).
E-mail addresses: starold@mdanderson.org (S.T. Arold), yves.collette@inserm.fr (Y. Collette), morelli@ifr88.cnrs-mrs.fr (X. Morelli).
[1] These authors contributed equally to this work as senior authors.

0014-5793/$36.00 © 2012 Federation of European Biochemical Societies. Published by Elsevier B.V. All rights reserved.
http://dx.doi.org/10.1016/j.febslet.2012.05.017

such as the Src tyrosine kinase which has been implicated in the ability of Alix to regulate cell surface receptor internalization and cell adhesion [9].

Crystal structures have revealed that human Alix is composed of three domains involved in multiple and diverse protein interactions: the N-terminal Bro1 domain (residues 1–358), that binds to ESCRT-I/III proteins [7,10], a central V domain (residues 362–702) that is formed by two three-helix bundles disposed in a "V" shape; and a C-terminal PRR (proline-rich region; residues 703–868) that is not present in the available crystal structures, that serves as a docking site for a number of proteins, including TSG101 and Src-homology (SH)3 domain-containing proteins [10,11].

We previously identified Alix as a novel hematopoietic cell kinase (Hck) SH3-binding protein by yeast two-hybrid screening using the SH3 domains of Src family kinases (SFKs) [12]. Identification of Src-related Hck as a novel Alix binding partner was particularly relevant given the implication of Hck in similar cellular and pathological functions, including adhesion, actin polymerization, and HIV-1 infection (for review, see [13]). We demonstrated that Alix binds to and activates Hck, and delineated the proline-rich (PxxP) motif of the Alix PRR involved in binding to Hck-SH3. In the same study, we demonstrated that Alix residues outside of the PxxP motif enhanced affinity and also possibly specificity for Hck-SH3, which was reminiscent of the tertiary binding mode used by the viral protein Nef-HIV-1 [14–16]. Interactions outside the PxxP motif are thought to enhance affinity and specificity for SH3 domains (for review, refer to [17]) as demonstrated by the high affinity binding of the viral Nef protein to Hck SH3 domain which implicates a well-defined hydrophobic pocket formed by two α-helices of Nef [14]. In addition to the canonical PXXP motif, this pocket provides a three-dimensional 'tertiary' binding surface which has not been described so far for cellular proteins. We thus investigated in the current research, on the mode of binding of Alix to Hck-SH3 domain by combining ITC, NMR, SAXS and molecular modeling experiments and compared it to that of HIV-1 Nef.

2. Materials and methods

2.1. DNA construction

Human Alix recombinant construct ($ALIX_{V+PRR}$) consisting of residues 362–760 was prepared as previously described [12]. Wild-type Fyn-SH3 ($Fyn_{(WT)}$-SH3) and $Fyn_{(R96I)}$-SH3 sequences were amplified from pGEX-$Fyn_{(WT)}$ and pGEX-$Fyn_{(R96I)}$ plasmid constructs, respectively, and cloned into pET42a expression vectors using NdeI and XhoI restriction sites. Each construct was verified by DNA sequencing.

2.2. Yeast two-hybrid (Y2H)screen

Two independent yeast two-hybrid (Y2H) were performed in parallel, using the human Hck- or $Fyn_{(R96I)}$-SH3 domain as a bait. Y2H system is based on the protocol described by Walhout et al. [18] as described in Materials and Methods in the Supporting Information.

2.3. Protein expression

Human Alix recombinant construct ($ALIX_{V+PRR}$) was expressed with an N-terminal His_6-Smt3 fusion tag in *Escherichia coli* strain BL21 (DE3). The different SH3 recombinant proteins ($Fyn_{(WT)}$-SH3, $Fyn_{(R96I)}$-HS3, and Hck-SH3) were similarly expressed as 6xHis C-terminal fusion proteins in *E. coli* BL21 (DE3). The different recombinant proteins ($ALIX_{V+PRR}$ and SH3 protein) were expressed and purified as described in Materials and Methods in the Supporting Information.

2.4. Isothermal titration calorimetry (ITC)

ITC was used to evaluate the thermodynamics parameters of the binding between $ALIX_{PI}$ peptide and $Fyn_{(WT)}$-SH3 or $Fyn_{(R96I)}$-SH3. Titrations were carried out at 25 °C on a MicroCal ITC200 microcalorimeter (GE Healthcare, Piscataway, NJ). Experiments and data analysis were performed as described in Materials and Methods in the Supporting Information.

2.5. NMR spectroscopy

To further elucidate the interaction mode between the SH3 domains and $ALIX_{V+PRR}$, ^1H–15N heteronuclear single quantum coherence (HSQC) experiments were performed as described in Materials and Methods in the Supporting Information.

2.6. Small-angle X-ray scattering (SAXS) analysis

Data used for the SAXS analysis of the complex between $Fyn_{(R96I)}$ and $ALIX_{V+PRR}$ were collected at the SWING beamline of the SOLEIL synchrotron in Paris, France, as described in more details in Materials and Methods in the Supporting Information.

2.7. Peptide docking studies

Docking of Alix peptide onto $Fyn_{(R96I)}$-SH3 and $Fyn_{(WT)}$-SH3 mutants was performed using the high-resolution modeling protocol provided by FlexPepDock [19]. The Fyn $Fyn_{(R96I)}$-SH3:HIV-1 Nef crystal structure (PDB ID 1EFN [14]) was used as a template for $Fyn_{(R96I)}$-SH3. $Fyn_{(WT)}$-SH3 was obtained by replacing I96 with an arginine (in its most common rotamer). The initial Alix peptide structure was obtained by computationally mutating and extending the Nef PXXP motif from the pdb template. FlexPepDock was set up to produce 300 low resolution and 300 high resolution structures. Produced models reached peptide backbone r.m.s.d. of more than 10 Å compared to the initial peptide structure, showing that the flexible docking procedure was not only exploring local minima.

3. Results and discussion

3.1. Isoleucine 92 from the Haemopoietic cell kinase RT-loop is involved in the specific recognition of $ALIX_{V+PRR}$

The so-called "tertiary" mode of recognition used by HIV-1 Nef to selectively target SH3 domains is provided by the folded core domain of the protein [14,16]. In addition to binding mediated by the PPII helix, an isoleucine residue from the RT loop of the Hck SH3 domain (I92) inserts into a well-defined hydrophobic pocket formed by two α-helices of Nef. The corresponding residue in Fyn SH3 RT loop is an arginine (R96) which leads to a low affinity binding to Nef (K_d > 20 μM), whereas its substitution by an isoleucine (R96I) converts the Fyn SH3 domain from a low to a high affinity ($K_d \approx 0.4$ μM) binding partner for Nef [15]. This selective mode of recognition mediated by HIV-1 Nef was reproduced in a yeast two hybrid assay, as shown in Supplementary Fig. S1A. Co-transformation of cells with Nef resulted in β-Galactosidase production and yeast outgrowth on media lacking uracil for Hck-SH3 and $Fyn_{(R96I)}$-SH3 as baits, but not for $Fyn_{(WT)}$-SH3. These results were confirmed using the *lacz* and *his3* reporters for Nef:Hck-SH3 and Nef:$Fyn_{(WT)}$-SH3 (because $Fyn_{(R96I)}$-SH3 alone was able to transactivate the *lacz* and *his3*, $Fyn_{(R96I)}$-SH3 could not be used with these reporter systems). In contrast to HIV-1 Nef, the Src-associated in mitosis 68 kDa (SAM68) protein interacted with comparable strength with every SH3 domain, indicating that the architecture

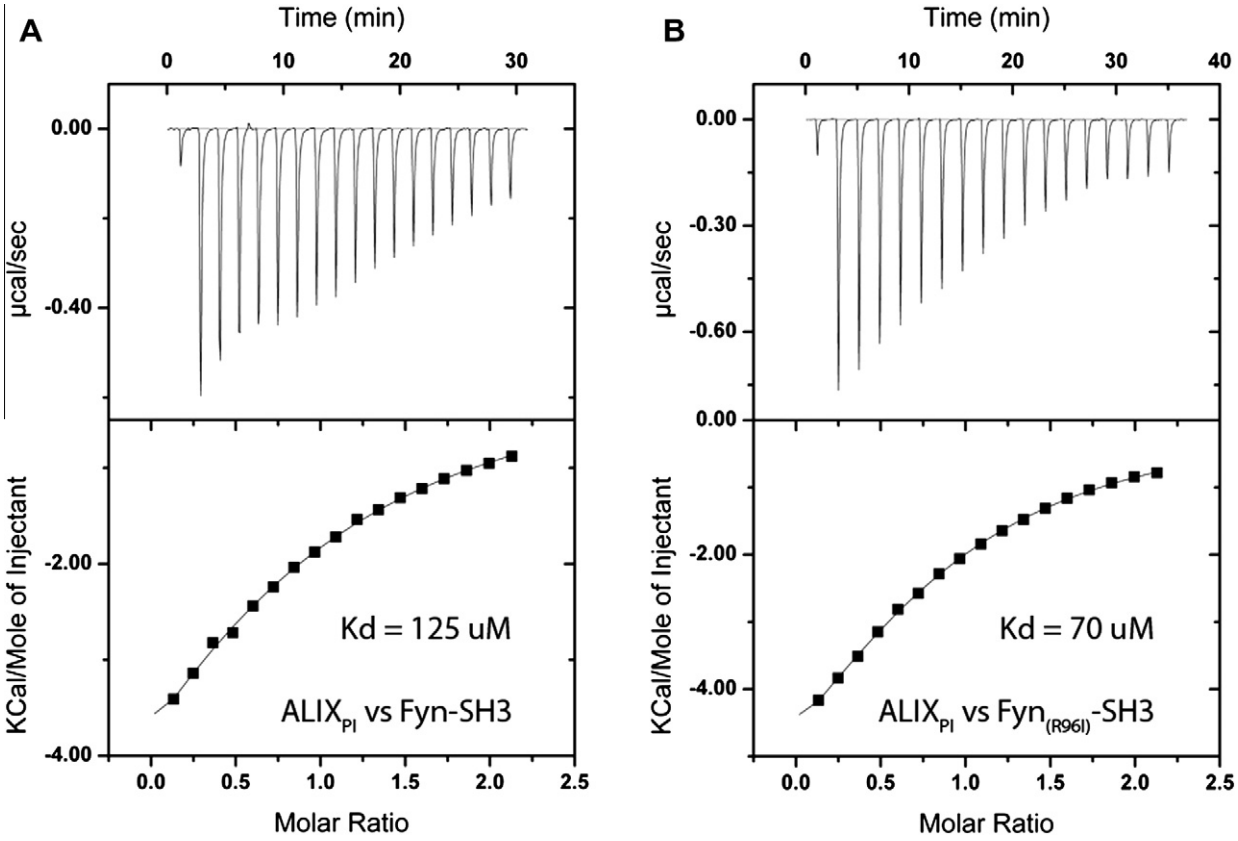

Fig. 1. (A, B) Experimental ITC binding curves for the interaction between $ALIX_{PI}$ and (A) $Fyn_{(wt)}$-SH3, (B) $Fyn_{(R96I)}$-SH3. Top panel: Raw ITC data from an experiment. Bottom panel: Non-linear least-squares fit of the data from the top panel after blank subtraction.

of the SAM68 binding site cannot produce a Nef-like SH3 selection of the RT-loop amino acid position 96 (negative control).

Next, we analyzed the interaction between these SH3 domains and an Alix fragment encoded by one Alix clone, called IIIA9, obtained in a yeast two hybrid screening using the Hck SH3 domain as bait [12]. This Alix fragment contained the Hck-interacting proline-rich region (PRR) as well as part of the Alix V domain (alignment details in Supplementary Fig. S1C), suggesting that these two regions of the Alix V domain contribute to Hck SH3 binding, which was reminiscent of the Nef binding mode of action (Supplementary Fig. S1B).

To confirm the "Nef-like" binding selectivity for the RT-loop position 92 in vitro, we carried out GST pull-down experiments followed by SDS–PAGE and Coomassie blue staining. These experiments illustrate the binding of an Alix fragment encoding for the V domain and the SH3-binding PRR motif ($Alix_{V+PRR}$) to Hck-SH3-GST and $Fyn_{(R96I)}$-SH3-GST but not to $Fyn_{(WT)}$-SH3-GST (Supplementary Fig. S2). Thus, the recombinant $ALIX_{V+PRR}$ could differentiate SH3 domains according to their amino acids at position 92 (or 96 for Fyn), displaying a "Nef-like" selectivity in vitro.

3.2. Molecular recognition mode does not involve a 3D fingerprint but rather demonstrates an extended linear pattern

Next, we asked whether the $ALIX_{V+PRR}$-SH3 binding site was demonstrating a structurally similar binding site to the one observed for HIV-1 Nef protein. For Nef, the tertiary SH3 recognition binding site is formed by the Nef PRR and part of the folded Nef core domain [14,16]. In contrast, sequence analysis and secondary structure prediction indicates that the Alix PRR is located within an unstructured region, 35 residues away from the folded V domain (Supplementary Fig. S3). The location of the Alix PRR in an unstructured region is consistent with our previous SAXS data for apo-$ALIX_{V+PRR}$ [12]. We, and others, previously published ITC experiments indicating that the affinity and thermodynamic parameters of the Nef/Hck-SH3 interaction were dramatically different from those of the interaction between Hck-SH3 and the Nef PRR peptide [15,20]. Similarly, previous ITC experiments for the Alix/Hck-SH3 complex demonstrated that a peptide containing the minimal Alix PxxP consensus motif ($ALIX_{PI}$, residues 737–760) did not fully reproduce the binding characteristics of $ALIX_{V+PRR}$ toward Hck-SH3; however, inclusion of residues N-terminal to the PxxP consensus motif in the peptide sequence almost completely restored the binding characteristics of $ALIX_{V+PRR}$ [12]. In the present study, we demonstrate that the isolated peptide $ALIX_{PI}$ is also capable of distinguishing between $Fyn_{(WT)}$-SH3 (K_d = 160 ± 30 μM) and $Fyn_{(R96I)}$-SH3 (K_d = 54 ± 10 μM), and that $ALIX_{PI}$ binds to each SH3 domain with K_d's similar to those observed with $ALIX_{V+PRR}$ (please refer to Fig. 1A and B for the peptide $ALIX_{PI}$ in complex with $Fyn_{(WT)}$-SH3 or $Fyn_{(R96I)}$-SH3 experiments, to compare with [12] for the peptide $ALIX_{PI}$ or $ALIX_{V+PRR}$ in complex with Hck-SH3 experiment). These results suggest that if a tertiary 'Nef-like' binding occurs, its thermodynamic fingerprint is weak. Also, our previous NMR studies failed to show a significant difference between the imprints of $ALIX_{V+PRR}$ and the Alix PRR peptide on Hck-SH3, and hence they failed to reveal a clear indicator of a tertiary 3D binding site [12]. Therefore, we used NMR to investigate whether the imprint of $ALIX_{V+PRR}$ on the different SH3 domains varies with their origin or affinity.

NMR HSQC experiments with ^{15}N-labelled Hck-SH3, $Fyn_{(WT)}$-SH3, and $Fyn_{(R96I)}$-SH3 in the presence of 1 equiv. of unlabelled $ALIX_{V+PRR}$ showed that the chemical shifts induced by $ALIX_{V+PRR}$ mapped to almost the same residues on the surfaces of all SH3 domains, including the low-affinity $Fyn_{(WT)}$-SH3 domain (Fig. 2A–C).

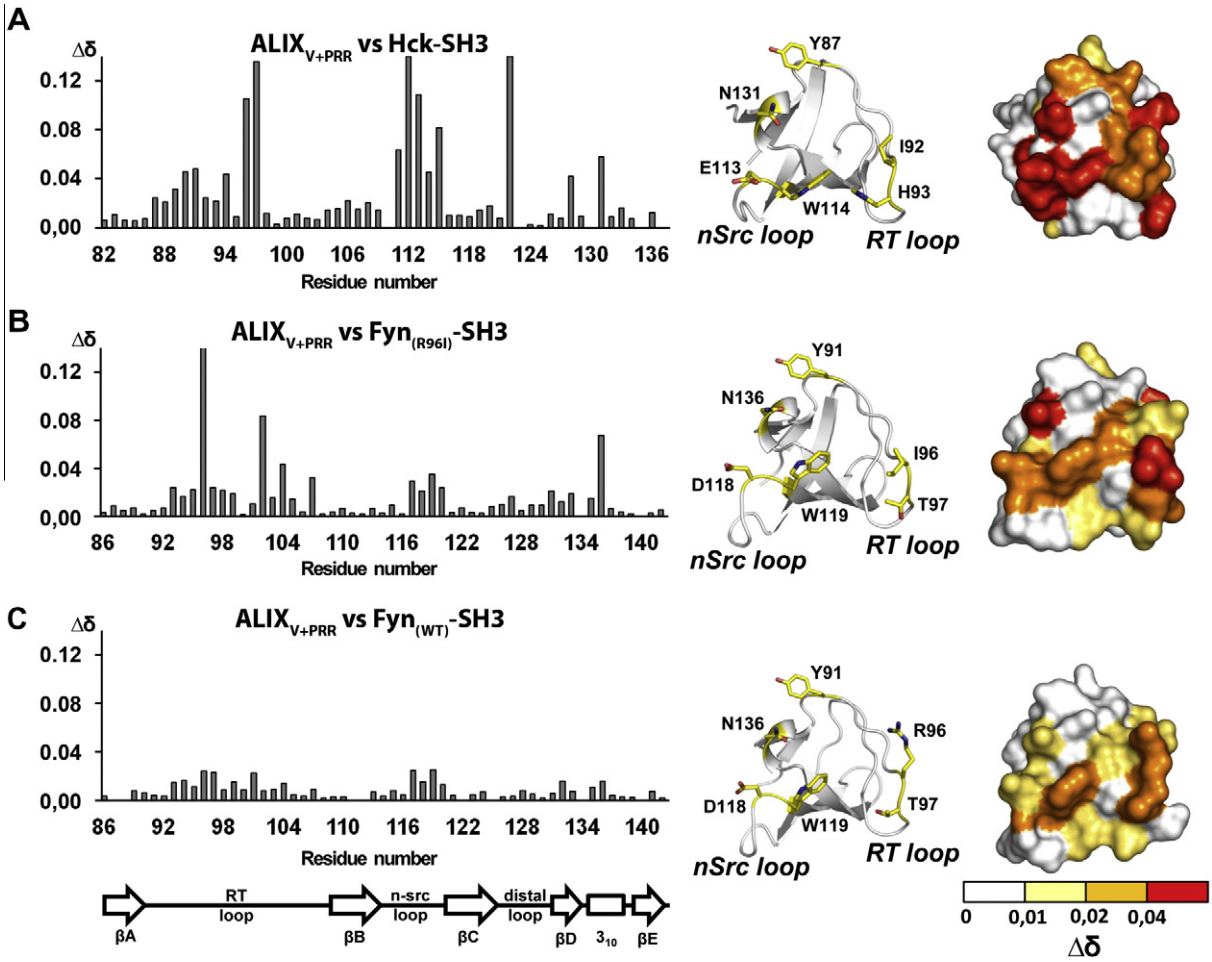

Fig. 2. Mapping of the SH3 domains' atomic recognition surfaces in the presence of ALIX$_{V+PRR}$ by heteronuclear NMR. (A–C) Left: SH3 residues' chemical shifts observed for (A) Hck-SH3, (B) Fyn$_{(R96I)}$-SH3, and (C) Fyn$_{(WT)}$-SH3 in the presence of 1 equiv. of ALIX$_{V+PRR}$, shown as histograms. The relative variations of ^{1}H and ^{15}N were calculated according to Grzesiek et al. [22]. Center: Ribbon representation of the different SH3 domains with important interacting residues in yellow for (A) Hck-SH3, (B) Fyn$_{(R96I)}$-SH3, and (C) Fyn$_{(WT)}$-SH3 (PDB entries 1BU1, 1EFN, and 1AVZ, respectively). Right: Corresponding chemical shifts of the SH3 proteins in the presence of 1 equiv. of ALIX$_{V+PRR}$, shown as a surface representation onto the SH3 domain structures. Small chemical shift variations are represented in yellow, larger shifts in orange, and the largest in red.

For all SH3 domains tested, markedly affected residues were distributed over four regions of the SH3 domain—the RT loop, the nSrc loop, the 3_{10} helix, and the canonical hydrophobic grooves (Fig. 2A)—in agreement with the results of our previous study of ALIX$_{V+PRR}$ binding to Hck-SH3 [12]. Of note, the intensity of the chemical shift increased remarkably, as expected, with the K_d observed (using strictly the same, 1 equiv. amount of ALIX$_{V+PRR}$ in all experiments). Although the imprints are similar globally, subtle differences can be observed in the surface area of the residues involved in the recognition process; for example, the nSrc loop seems to be more involved in the Hck-SH3–ALIX$_{V+PRR}$ interaction than in the Fyn$_{(R96I)}$-SH3–ALIX$_{V+PRR}$ interaction (Fig. 2A–C). Nonetheless, the overall interaction mode is similar enough for all SH3 proteins to indicate a structurally similar engagement of all three SH3 domains by ALIX$_{V+PRR}$. Also, the extent of the binding surface on SH3 domains is compatible with an ALIX$_{V+PRR}$ binding mode that has a linear "peptide-like" interaction rather than a 'Nef-like' 3D interaction.

3.3. Molecular model of the SH3-ALIX$_{V+PRR}$ complex

To corroborate that the PRR in ALIX$_{V+PRR}$ does not join the V domain to form a 'Nef-like' tertiary SH3 binding site upon SH3 engagement, we used SAXS. Ensemble Optimization Method (EOM) reconstructions showed that the PRR-bound Fyn$_{(R96I)}$-SH3 was highly flexible and had a large, variable distance from the V domain core (Fig. 3A and B). The maximum diameter (D_m) calculated from the SAXS data for Fyn$_{(R96I)}$-SH3-bound ALIX$_{V+PRR}$ (D_m = 190 ± 10 Å) was the same as the D_m value we measured previously for apo-ALIX$_{V+PRR}$ [12]. These results argue against a model in which the SH3 binding motif in the flexible region C-terminal to the Alix V domain folds back onto the V domain to form a combined tertiary SH3 site.

Together, our data indicate that Alix achieves a 'Nef-like' RT-loop selection through a linear "peptide-like" binding mode rather than through a 'Nef-like' tertiary SH3 recognition mode. Hence, the observed differences in the Y2H and K_d, especially between Fyn$_{(WT)}$-SH3 and Fyn$_{(R96I)}$-SH3, must be explained by differences in the interaction between the Alix PRR sequence and the SH3 RT loops. All attempts to crystallize Fyn$_{(R96I)}$-SH3 in a complex with Alix PRR failed, because all crystals packing involve homologous interactions between PxxP-motif binding sites of the SH3 domain. We therefore used the high-resolution docking and refinement protocol FlexPepDock [19] to model SH3–peptide complexes. FlexPepDock is implemented within the ROSETTA framework, which has proven its high accuracy in several landmark modeling successes. The obtained Fyn$_{(R96I)}$-SH3/ALIX$_{PI}$ and Fyn$_{(WT)}$-SH3/ALIX$_{PI}$ structures provide a possible explanation for how a linear sequence can distinguish between R96 and I96. These structures show that in addition to the canonical interaction between Fyn

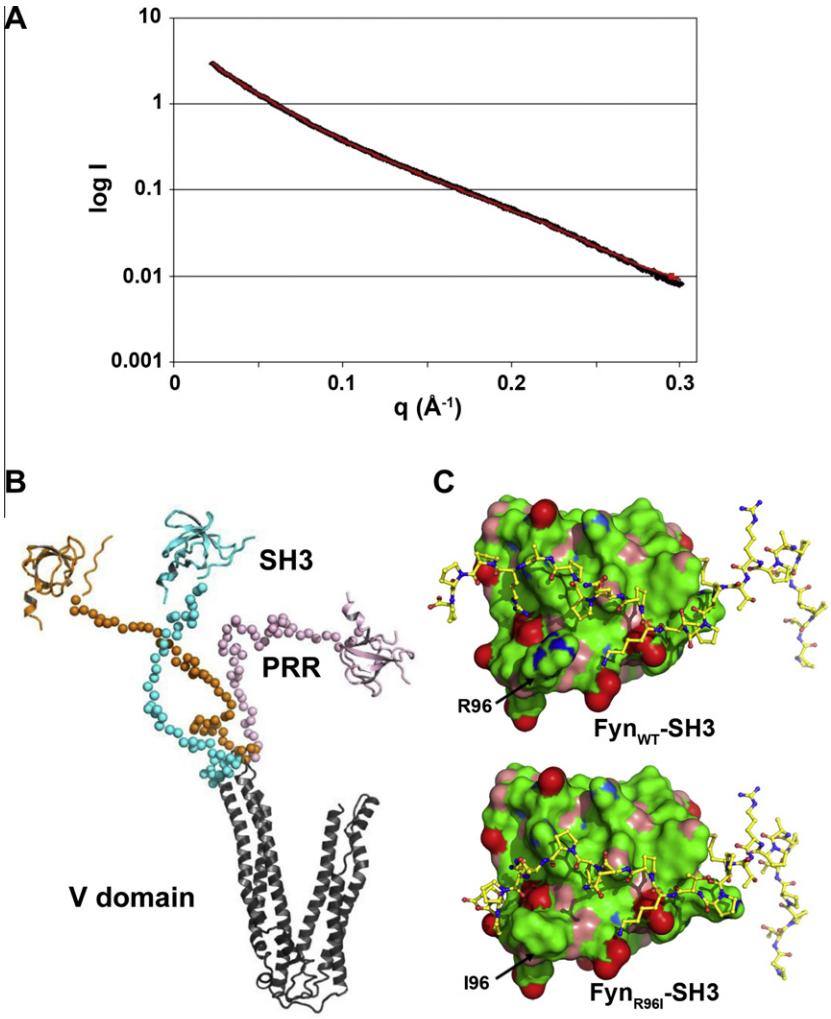

Fig. 3. SAXS model of $ALIX_{V+PRR}$ complexed to $Fyn_{(R96I)}$-SH3. (A) Fit of EOM SAXS ensemble model (red) to data (black). (B) Three representative structural models taken from an ensemble of 15 structures produced by EOM on the basis of SAXS data, superimposed on their Alix V domain (black ribbon). $ALIX_{V+PRR}$-bound $Fyn_{(R96I)}$-SH3 (represented as secondary structures) and flexible residues (represented as spheres) linking the Alix PRR to the V domain have a different color for each model. (C) Alix peptide/$Fyn_{(R96I)}$-SH3 (top) and Alix peptide/$Fyn_{(WT)}$-SH3 (bottom) 3D interaction models obtained from Flexpepdock. SH3 domains are oriented as in Fig. 2. SH3 surfaces are colored according to blue, positively charged atoms; red, negatively charged atoms; green, hydrophobic atoms; salmon, polar oxygens; light blue, polar nitrogens; yellow, sulfur. The Alix peptide is shown as a stick model.

D100 and Alix R757, the I96 of $Fyn_{(R96I)}$-SH3 may establish favorable hydrophobic interactions with $ALIX_{PI}$ prolines 754, 758–759 (Fig. 3C). These favorable proximity of hydrophobic residues is not possible with R96 of $Fyn_{(WT)}$-SH3. In addition, the proximity of the positive charge of R96 may also decrease the strength of an interaction between Fyn E94 and $ALIX_{PI}$ K751. E94 is conserved in Hck-SH3, and FlexPepDock analysis suggests that this E94–$ALIX_{PI}$ K751 interaction is conserved in Hck (data not shown). Our docking analysis also provides a possible explanation for our previous observation that the minimal Alix PxxP consensus does not fully reproduce the binding of $ALIX_{V+PRR}$ [12], by suggesting that Alix M747 (which was not included in the minimal Alix PxxP peptide) engages a hydrophobic interaction with an apolar pocket formed by Fyn-SH3 L90 and Y91.

4. Conclusion

Our results indicate that ALIX achieves a 'Nef-like' RT-loop selection through an extended linear "peptide-like" binding mode rather than through a 'Nef-like' tertiary SH3 recognition mode. Our binding studies and computational modeling analysis suggest a molecular basis for how the extended linear interaction of ALIX with Hck-SH3 is capable of reproducing the 3D 'tertiary' binding mode of HIV-1 Nef without a 3D organization. Together with the observation that linear SH3-binding motifs can bind to SH3 domains with similar affinities than does HIV-1 Nef [21], this opens the question why Nef uses a costly three-dimensional framework for SH3 binding if a much simpler linear recognition motif achieves the same affinity and specificity.

Funding

This work was supported by the Centre National de la Recherche Scientifique (CNRS); the Institut National de la Santé et de la Recherche Médicale (INSERM); the Agence Nationale de Recherche sur le SIDA et les hépatites virales (ANRS); the Ministry of Science and Technology, China [Grant Nos. 2007CB914304; 2006AA02A313]; the National Natural Science Foundation of China (NSFC) [Grant Nos. 30800181; 30625011]; the Research Foundation Flanders (FWO); the concerted action programme of the Katholieke Universiteit Leuven; and the National Institutes of Health (MD Anderson's Cancer Center Support) [Grant No. CA016672]. S.O. and A.L. were fellows of the ANRS, and X.S. was a fellow of the 'Ambassade de France en Chine'.

Acknowledgements

We thank Olivier Bornet for performing the NMR recording experiments, Marielle Beauzan for bacterial expression, Dieter Vermeire for Biacore support, Karen Muller for editorial assistance, Pascal Verdié for peptide synthesis and Javier Perez for support and setup of the SAXS beamline at the SOLEIL synchrotron in Paris, France.

Appendix A. Supplementary data

Supplementary data associated with this article can be found, in the online version, at http://dx.doi.org/10.1016/j.febslet.2012.05.017.

References

[1] Chatellard-Causse, C., Blot, B., Cristina, N., Torch, S., Missotten, M. and Sadoul, R. (2002) Alix (ALG-2-interacting protein X), a protein involved in apoptosis, binds to endophilins and induces cytoplasmic vacuolization. J. Biol. Chem. 277, 29108–29115.
[2] Pan, S. et al. (2006) Involvement of the conserved adaptor protein Alix in actin cytoskeleton assembly. J. Biol. Chem. 281, 34640–34650.
[3] Schmidt, M.H., Hoeller, D., Yu, J., Furnari, F.B., Cavenee, W.K., Dikic, I. and Bögler, O. (2004) Alix/AIP1 antagonizes epidermal growth factor receptor downregulation by the Cbl-SETA/CIN85 complex. Mol. Cell. Biol. 24, 8981–8993.
[4] Katoh, K., Shibata, H., Suzuki, H., Nara, A., Ishidoh, K., Kominami, E., Yoshimori, T. and Maki, M. (2003) The ALG-2-interacting protein Alix associates with CHMP4b, a human homologue of yeast Snf7 that is involved in multivesicular body sorting. J. Biol. Chem. 278, 39104–39113.
[5] Matsuo, H. et al. (2004) Role of LBPA and Alix in multivesicular liposome formation and endosome organization. Science 303, 531–534.
[6] Trioulier, Y., Torch, S., Blot, B., Cristina, N., Chatellard-Causse, C., Verna, J.M. and Sadoul, R. (2004) Alix, a protein regulating endosomal trafficking, is involved in neuronal death. J. Biol. Chem. 279, 2046–2052.
[7] Strack, B., Calistri, A., Craig, S., Popova, E. and Göttlinger, H.G. (2003) AIP1/ALIX is a binding partner for HIV-1 p6 and EIAV p9 functioning in virus budding. Cell 114, 689–699.
[8] Odorizzi, G. (2006) The multiple personalities of Alix. J. Cell Sci. 119, 3025–3032.
[9] Schmidt, M.H., Dikic, I. and Bögler, O. (2005) Src phosphorylation of Alix/AIP1 modulates its interaction with binding partners and antagonizes its activities. J. Biol. Chem. 280, 3414–3425.
[10] Lee, S., Joshi, A., Nagashima, K., Freed, E.O. and Hurley, J.H. (2007) Structural basis for viral late-domain binding to Alix. Nat. Struct. Mol. Biol. 14, 194–199.
[11] Fisher, R.D., Chung, H.Y., Zhai, Q., Robinson, H., Sundquist, W.I. and Hill, C.P. (2007) Structural and biochemical studies of ALIX/AIP1 and its role in retrovirus budding. Cell 128, 841–852.
[12] Shi, X. et al. (2010) Identification and biophysical assessment of the molecular recognition mechanisms between the human haemopoietic cell kinase Src homology domain 3 and ALG-2-interacting protein X. Biochem. J. 431, 93–102.
[13] Guiet, R., Poincloux, R., Castandet, J., Marois, L., Labrousse, A., Le Cabec, V. and Maridonneau-Parini, I. (2008) Hematopoietic cell kinase (Hck) isoforms and phagocyte duties – from signaling and actin reorganization to migration and phagocytosis. Eur. J. Cell Biol. 87, 527–542.
[14] Lee, C.H., Saksela, K., Mirza, U.A., Chait, B.T. and Kuriyan, J. (1996) Crystal structure of the conserved core of HIV-1 Nef complexed with a Src family SH3 domain. Cell 85, 931–942.
[15] Lee, C.H., Leung, B., Lemmon, M.A., Zheng, J., Cowburn, D., Kuriyan, J. and Saksela, K. (1995) A single amino acid in the SH3 domain of Hck determines its high affinity and specificity in binding to HIV-1 Nef protein. EMBO J. 14, 5006–5015.
[16] Arold, S., Franken, P., Strub, M.P., Hoh, F., Benichou, S., Benarous, R. and Dumas, C. (1997) The crystal structure of HIV-1 Nef protein bound to the Fyn kinase SH3 domain suggests a role for this complex in altered T cell receptor signaling. Structure 5, 1361–1372.
[17] Li, S.S. (2005) Specificity and versatility of SH3 and other proline-recognition domains: structural basis and implications for cellular signal transduction. Biochem. J. 390, 641–653.
[18] Walhout, A.J. and Vidal, M. (2001) High-throughput yeast two-hybrid assays for large-scale protein interaction mapping. Methods 24, 297–306.
[19] London, N., Raveh, B., Cohen, E., Fathi, G. and Schueler-Furman, O. (2011) Rosetta FlexPepDock web server – high resolution modeling of peptide–protein interactions. Nucleic Acids Res. 39, W249–W253.
[20] Arold, S., O'Brien, R., Franken, P., Strub, M.P., Hoh, F., Dumas, C. and Ladbury, J.E. (1998) RT loop flexibility enhances the specificity of Src family SH3 domains for HIV-1 Nef. Biochemistry 37, 14683–14691.
[21] Ladbury, J.E. and Arold, S.T. (2011) Energetics of Src homology domain interactions in receptor tyrosine kinase-mediated signaling. Methods Enzymol. 488, 147–183.
[22] Grzesiek, S. et al. (1996) The solution structure of HIV-1 Nef reveals an unexpected fold and permits delineation of the binding surface for the SH3 domain of Hck tyrosine protein kinase. Nat. Struct. Biol. 3, 340–345.